

# The design guidelines for the permanent magnet synchronous motors for fan and pump drives

The algorithm for determining the optimal working point of electric drives for fan and pump systems has been developed. The procedure allows to calculate the fan or pump generated full-load characteristic of the driving motor. The algorithm of preliminary design of permanent magnet synchronous motor for such type of drives has been proposed. It can be used to define the set of initial points in the permanent magnet motor optimization processes. The algorithm and computer software for the cogging torque minimization has been also developed.

## 1. Introduction

Electric drives for ventilation and drainage systems used in mining industry represent significant part of all electric drives. Thousands of electric motors with power ranging from just a few kilowatts to several megawatts are used in the ventilation systems. The second most power consuming systems are the drainage systems in which mainly the impeller pumps are employed pumps. Overall power usage of these systems in the mining industry in Poland can be counted in gigawatts. Proper design of the drives and the control systems is crucial to minimize energy consumption in this sector.

Asynchronous drives are usually used in these two systems, with the exception of the most powerful fan drive applications, where synchronous motors are employed. It can be observed, however, that the nowadays the tendency to use synchronous motors for the less power demanding applications is becoming more popular. Permanent magnet synchronous motors using high-energy magnets made with neodymium-iron-boron (ND-Fe-B) alloy, are particularly effective in these applications. The constant angular speed ensures constant air or liquid flow rate in any given period of time. Such drives have also higher power coefficient and have greater energy efficiency due to lack of power loss in the rotor.

Use of the variable-speed drives is the most efficient way to control the air or liquid flow. Control systems for synchronous motors are much simpler than those used to control asynchronous drives. Prior to design of efficient synchronous motor and its control system it is necessary to determine load characteristics of fan or pump, i.e. the relation between the torque and angular speed.

In modern design processes of electromagnetic devices the optimization procedures, especially genetic, particle swarm or evolutionary algorithms are often employed. In these algorithms it is usually necessary to define the set of initial points (particles, individuals). Points in  $n$ -dimensional space correspond to various options of the designed object described by  $n$ -design variables. The convergence of the optimization process strongly depends on the selection of the proper initial variants (i.e. initial dimensions of the design device). The

---

<sup>1</sup>) prof. dr hab. inż., Instytut Elektrotechniki Elektroniki Przemysłowej, Politechnika Poznańska, ul. Piotrowo 3a, 60-965 Poznań, tel. +48 61 665 23 80,

<sup>2</sup>)

designer intuition plays important role in this process. At this stage of the optimal design process, the collection of relatively simple rules can also be helpful.

The size of each electric motor is determined by the following two basic dimensions: stator internal diameter  $D$  and so called idealized stator core length  $L_i$ . The product  $D^2 L_i$  determines the stator inner space volume and it is approximately equal to the rotor volume. It is well known that this product is approximately proportional to the motor rated electromagnetic torque. This statement is the starting point in designing of the motor, i.e. determination of the motor main dimensions:  $D$  and  $L_i$ . Other main parameters, e.g. stator external diameter, depend on the number of poles and the rated voltage. Determination of permanent magnet synchronous motor stator main dimensions however, requires minimization of the cogging torque in addition to rated and start-up parameters.

The rotor dimensions, especially the permanent magnets dimensions, depend on: the number of pole pairs, the type of hard magnetic material used, the width of the air gap, stator magnetic circuit reluctance and permissible linear current density in the stator winding.

## 2. Determination of the working point of the ventilation system

The rated flow rate  $Q_N$  [ $\text{m}^3/\text{s}$ ] at rated speed  $n_N$  is the basic parameter characterizing the fan or pump. Value of the fan flow rate demand and characteristic of the ventilated system  $Q = Q(\Delta p)$ , where  $\Delta p$  is the differential pressure, must to be given prior to the fan system design process. The aerodynamic resistance of the ventilated objects strongly depends on the rate flow  $Q$ , therefore the characteristic  $Q = Q(\Delta p)$  is strongly nonlinear. This characteristic is usually presented in an inverted coordinate system, i.e.:  $\Delta p = f(Q)$  – Fig 1.

The characteristic of the turbo-machine (fan or pump) is also given in the same coordinate system. The pressure difference between the two sides of the fan decreases as a result of decreasing aerodynamic resistance of the ventilated system, i.e. with the flow  $Q$  increase. Fan characteristics  $\Delta p = f(Q)$  is decreasing function – Fig. 1.

The point of intersection of these two characteristics (point  $K_N$  in Fig. 1) determines the working conditions of the system fan-ventilated object, i.e. system source-load.

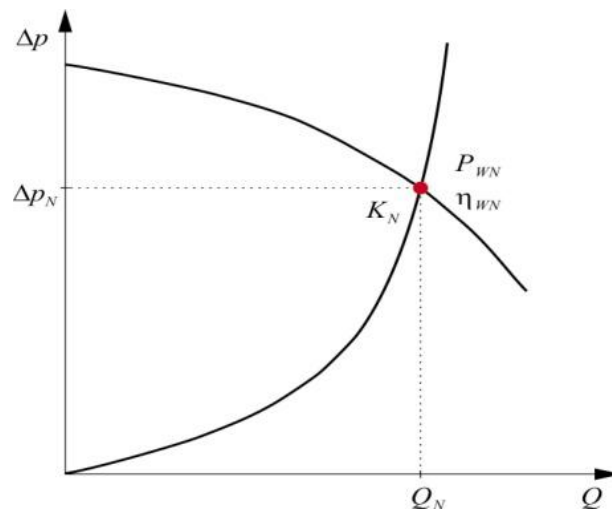


Fig. 1. Determination of the optimal working point of the system: fan-ventilated object.

Fan power output is equal to the product of differential pressure and flow rate values:  $P_w = \Delta p \cdot Q$  [5]. If  $Q = 0$  or  $\Delta p = 0$  then the power  $P_w = 0$ . This means, that there is an optimal working point  $K_{opt}(Q_{opt}, \Delta p_{opt})$  with the maximum fan output power – Fig. 2.

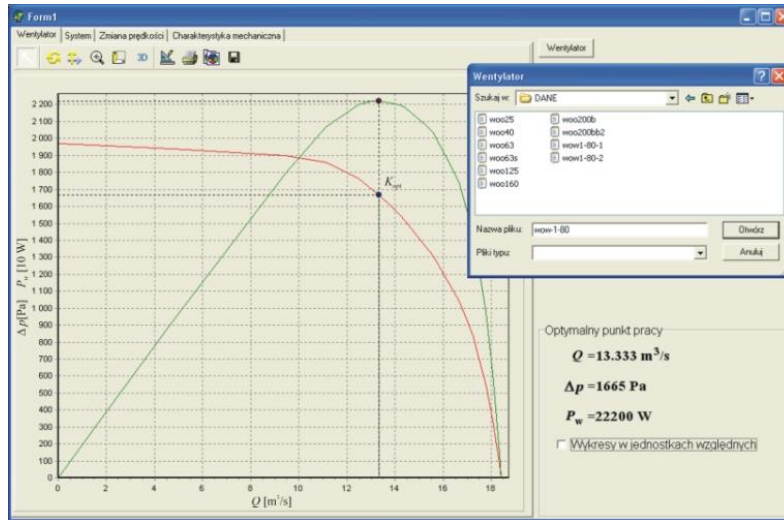


Fig. 2. Determination of the fan characteristics.

The motor rated power can be expressed as follows:

$$P_N = \frac{P_{wN}}{\eta_{wN}} = \frac{\Delta p_N \cdot Q_N}{\eta_{wN}} \quad (1)$$

and its rated torque:

$$T_N = \frac{P_{wN}}{\omega_N \cdot \eta_{wN}} = \frac{Q_N \cdot \Delta p_N}{\omega_N \cdot \eta_{wN}} \quad (2)$$

where  $\omega_N$ ,  $\eta_{wN}$  are the rated values of angular speed and efficiency, respectively.

The rated working point of selected fan should correspond to the maximum output power.

Rated power and rated torque of the driving electric motor can be determined on the basis of the relations (1) and (2).

### 3. Determination of full-load characteristics

Adjustment of the fan flow rate can be achieved by control of the motor angular speed. Flow rate of the fan at constant differential pressure is proportional to the speed and differential pressure at constant flow rate is proportional to the square of the speed [1,5], i.e.:

$$Q = \frac{\omega}{\omega_N} Q_N \quad \Delta p = \left( \frac{\omega}{\omega_N} \right)^2 \Delta p_N \quad (3)$$

Fan characteristic and optimal working point of the system for any angular speed that differs from rated value, can be calculated on the basis of relation (3). Figure 3 shows the set of the fan characteristics for  $\omega = \omega_N$  and  $\omega = 0,9; 0,8; 0,7; 0,6 \omega_N$ . Points of intersection of these curves and the characteristic of the ventilated object determine operating states (conditions) of the system at relevant speed values.

Assuming that the aerodynamic resistance is proportional to the speed and efficiency of the fan is speed independent than equations (3) show that the torque is proportional to the square of speed. In the real system, however, flow rate and differential pressure values change with variations of the angular speed of the fan. Relationship of these two parameters is highly nonlinear in relation to both: fan and ventilated system [1,5].

In order to determine the fan generated full-load characteristic  $T_m(\omega)$  of the driving motor the computer software has been developed. The software allows to determine set of fan characteristics for a selected range of speed and compute the set of operating points  $\{Q_i, \Delta p_i\}$  – Fig. 3. Points  $(\omega_i, T_{mi})$  of load characteristics are calculated according to the formula:

$$T_{mi} = \frac{Q_i \cdot \Delta p_i}{\omega_i} + m_0 \frac{Q_N \cdot \Delta p_N}{\omega_N} + \beta_t \frac{Q_N \cdot \Delta p_N}{\omega_N} \left( \frac{\omega_i}{\omega_N} \right)^q \quad (4)$$

where  $m_0 = \omega_N T_0 / Q_N \cdot \Delta p_N$  – relative static friction torque,  $\beta_t = \eta_{w/N}^{-1} - 1 - m_0$  – relative friction coefficient,  $q$  – exponent characterizing dependence of friction torque on speed.

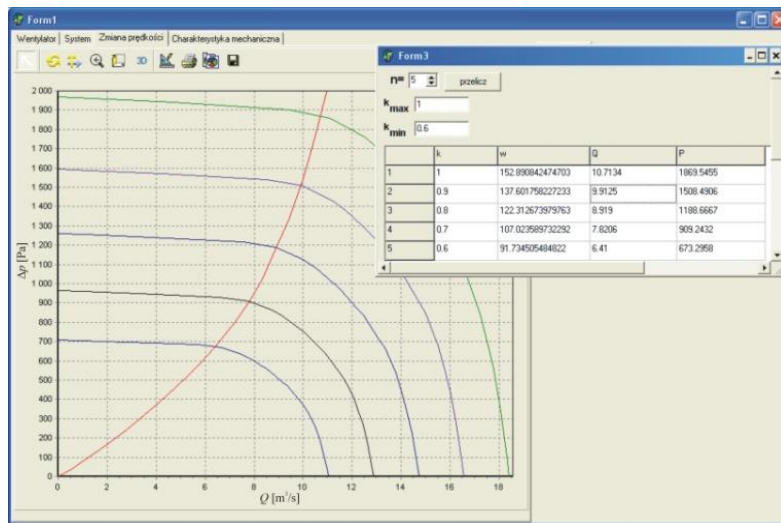


Fig. 3. Determination of characteristics for different angular speeds

An exemplary load characteristic constructed on the basis of equation (4) is shown in Fig. 4.

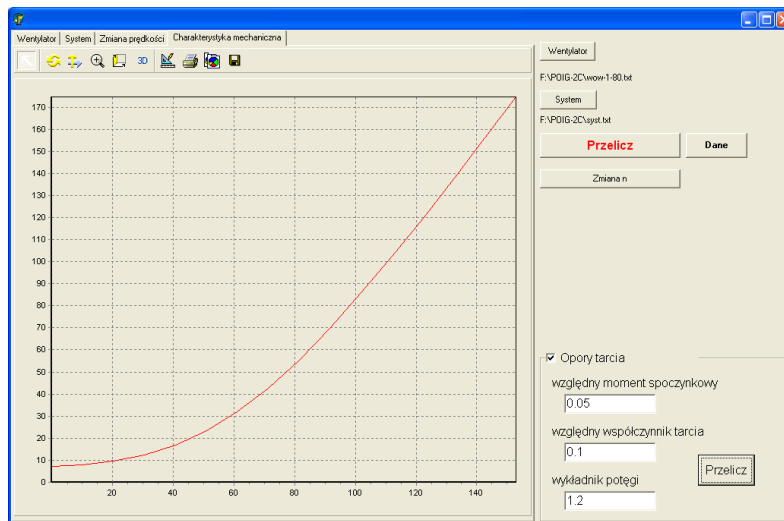


Fig. 4. Load characteristics  $T_m(\omega)$

#### 4. Determination of the rated torque and pump generated load characteristics of the driving motor

In the mining industry mainly the impeller (rotodynamic) pumps are employed. In the underground mines the pumps are used for drainage of mine faces and drawing levels. Drainage pumps up to 6 kW are used on the rock walls, pumps up to 20 kW are used for dewatering of mine faces. Units up to 90 kW are used for pumping water between the intermediate levels. Pumps with power output of more than 1 MW are used to extract water directly onto the surface (even more than 600 m). In strip mines pumps are used to active drainage and boreholes dewatering. [ ].

Operation of the impeller pump is very similar to the axial flow fan operation. It creates differential pressure between the inlet and the outlet of the pump. A characteristic aspect of the impeller pump is reverse flow of liquid after the pump stops, caused by the water column pressure. In such case the pump start-up is often done at considerable high initial load and therefore, the driving motor must have high starting torque. On the other hand, the inertia of the rotating parts of the pump is noticeable smaller than inertia of the comparable capacity fan and in this respect the pump start-up process is less demanding.

The basic parameter characterizing the pump is its rated output capability (i.e flow rate)  $Q_N$  [ $m^3/s$ ] at rated speed  $\omega_N$ . The other key parameters of the pump are: pressure expressed in height  $H$  of the water column (called the pump pressure head or elevating head or delivery head), power  $P$  and efficiency  $\eta$ . They are presented as a function of the pump flow rate  $Q$  and are called pump characteristics. The most important characteristic is dependence of the pump lifting head  $H$  on the flow rate  $Q$ , at constant angular speed. It is so called the throttle curve. This characteristic can be stable or non-stable – Fig. 6. Stable characteristic is monotonically descending curve and maximum of the pressure head  $H$  occurs at flow rate  $Q = 0$ . In the case of non-stable characteristics, the same value of pressure head  $H$  corresponds to two values of flow rate  $Q$ .

The pump installation consist of numerous components. Hydraulic losses  $\Delta H_r$  are caused by viscous friction between the liquid and the installation. System is characterized by the dependence of hydraulic losses (expressed in meters of height of water column) on the flow rate. These losses depend on the shape, diameter and length of pipes, type and dimension of valves and pipe fittings and, of course, on the velocity of flow. The operating point of the system is located at the intersection of pump and installation characteristics – Fig. 6. The pump pressure head  $H$  have to be equal to the sum  $\Delta H_r$  of hydraulic losses. If there is difference in level  $H_g$  between the beginning and the ending of the installation, than the pressure head  $H = H_g + \Delta H_r$  (8). Characteristics of the installation and the pump are shown in Fig. 5. Point  $B$  of intersection of these curves is the optimal working point of coordinates  $Q_p, H_p$ . If the hydraulic resistance of installation will increase, e.g. due to the pipe bend or connecting smaller diameter pipe, the optimal working point moves to point  $C$ . The pump lifting head will increase to the value  $H'_p$  and its flow rate will decrease to the value  $Q'_p$ .

Rated torque of the driving motor can be expressed as:

$$T_N = \frac{\gamma \cdot Q_N \cdot H_N}{\omega_N \cdot \eta_{pN}} \quad (5)$$

where:  $\gamma$  is the specific gravity of liquid.  $\omega_N$ ,  $\eta_{pN}$  are the rated angular velocity and rated pump efficiency, respectively.

Pump, in respect to the entire system, should be selected in such a way, that the nominal working point should close to the optimal point, which in turn corresponds to the maximum power output and the maximum efficiency of the pump.

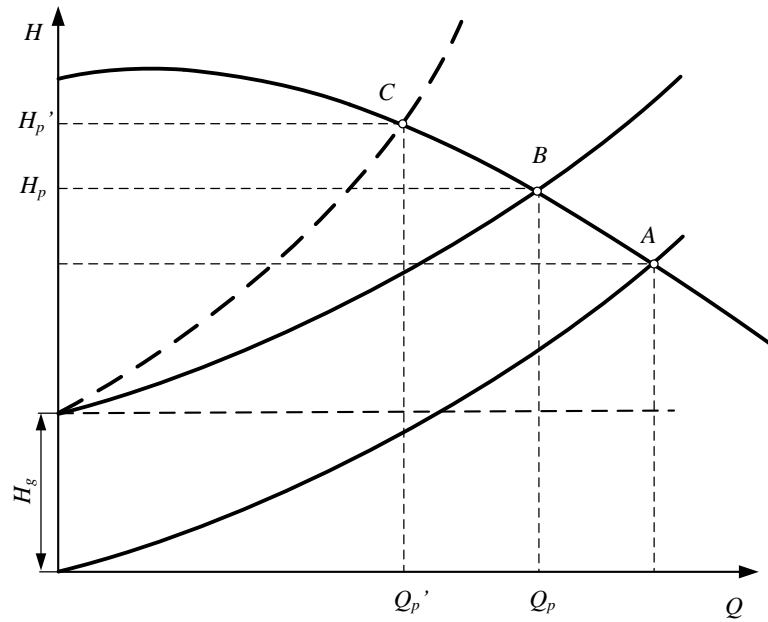


Fig. 5. Optimal working point of the system at constant speed, for different installation characteristics: (A) without initial pressure head; (B) with initial head  $H_g$  and (C) with initial head  $H_g$  and increased hydraulic resistance

The pump flow rate (at constant pressure head) is proportional to the angular speed and pressure head (at constant flow) is proportional to square of the speed. On that basis, the pump characteristics and the optimal working point for any speed  $\omega$  different than the rated value  $\omega_N$  can be determined. Fig. 8 shows the set of characteristics for  $\omega = \omega_N$  and  $\omega_1 < \omega_N$ ;  $\omega_2 < \omega_1$ . Points  $K_N, K_1, K_2$ , define the states of the system relevant to these speeds.

In the systems with variable speed the pump flow rate and pump pressure head vary freely with the change of the speed. Relationship between these parameters in respect to both: the pump and the installation is highly nonlinear.

The full-load characteristic  $T_m(\omega)$  of the pump can be calculated in similar way as in case of fan. generated by the pump the computer software has been developed. The software dedicated to this purpose has been developed. It allows to: enter data describing the pump and the installation, determine the optimal working point of system, determine the set of pump characteristics for selected range of speed (Fig. 9), determine the set  $\{Q_i, H_i\}$  of optimal working points for different speeds  $\omega_i$  and corresponding values of torque:

$$T_{mi} = \frac{\gamma \cdot Q_i \cdot H_i}{\omega_i \eta_{pi}} \quad (6)$$

The points calculated according to (6) allow to determine load characteristics  $T_m(\omega)$  – Fig. 6. The expression (6) is valid only for angular speeds  $\omega_i$  greater than critical value  $\omega_c$ , which corresponds to the point of intersection of the pump and installation curves at  $Q = 0$ .

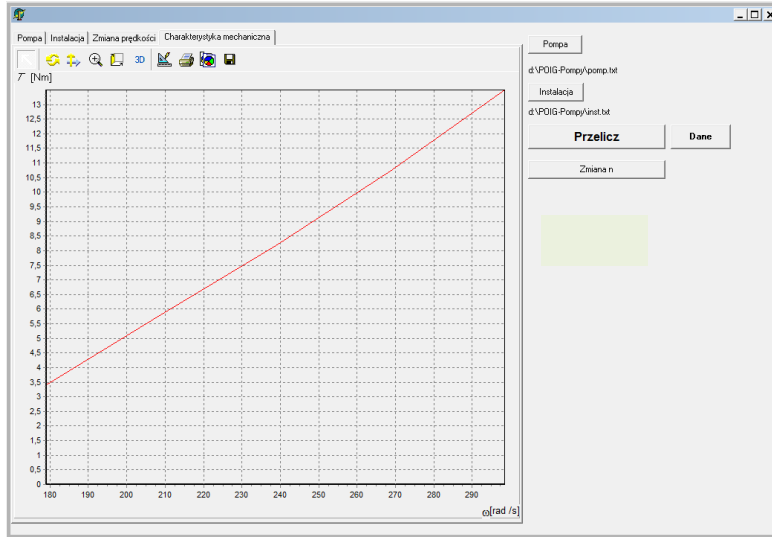


Fig. 6. Determination of load characteristics  $T_m(\omega)$  for freely various flow rate and pressure head

## 5. The initial selection of the permanent magnet excited motors main dimensions

Product  $D^2L_i = V_w$  determines active volume inside the stator. Almost from the beginning of the development of the design methods, in order to determine dimensions  $D$  and  $L_i$ , so-called machine-constants, e.g. Arnold's or Richter's constant, were used [1]. If these parameters are considered as truly constant numbers than electromagnetic torque of the machine is approximately proportional to the active volume, i.e.  $T = c_T V_w$ . In reality, these parameters depend (to a certain extent) on the size of the proposed machine, the rotational speed but mostly depend on the kind (quality) of used materials: conductive, ferromagnetic and insulating. In the case of permanent magnet excited motors constant  $c_T$  strongly depends on the type of hard magnetic material the permanent magnets are made of. The constant  $c_T$  can be estimated using e.g. the method of volume forces. Force acting on a single wire of the stator coil:  $f_\alpha = B_r J_z s_p L_i$ , where  $J_z$  is the current density in the wire,  $B_r$  is the radial component of magnetic flux density vector,  $s_p$  is the cross-section area of the wire. After integrating with respect to the whole winding area one obtains:

$$T = \frac{D^2 L_i}{4} g \cdot p \int_0^{\pi/p} \frac{B_r J_z}{2\mu_0} d\alpha \quad (7)$$

where  $g$  is a thickness of conducting layer, product  $a_z = gJ_z(\alpha)$  denotes the linear current density (called "specific electric loading") [1]. Taking an average value  $B_r \approx 0,5\text{T}$  and average value  $a_z \approx 50\text{kA/m}$ , which is typical for the machines with the power ranging from few to tens of kilowatts [1], the following constant can be derived:

$$c_T = \frac{p}{4} \int_0^{\pi/p} \frac{B_r(\alpha) a_z(\alpha)}{2\mu_0} d\alpha \approx (12 \div 16) \cdot 10^3 [\text{Nm/m}^3] \quad (8)$$

Data on a wide range of permanent magnet excited motors has been collected in [4, 5]. Fig. 7 shows dependence of the volume  $V_w = D^2 L_i$  on the rated torque  $T_N$  of motors using NdFeB magnets (curve 1) and ferrite magnets (curve 2).

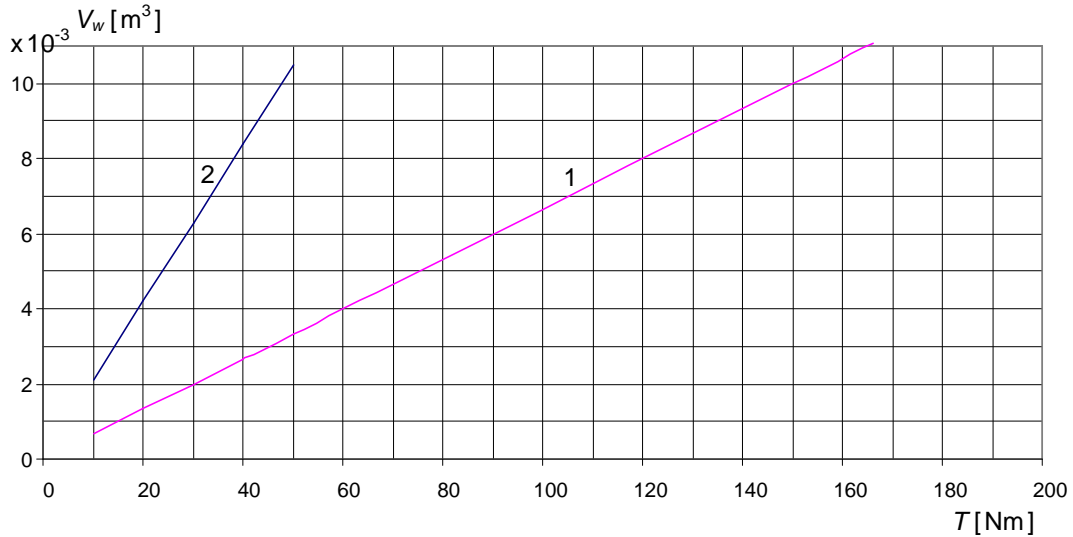


Fig. 7. Dependence of the volume  $V_w = D^2 L_i$  on the rated torque of motors using NdFeB magnets (curve 1) and ferrite magnets (curve 2).

Fig.7 can be useful in determination of the proportionality constant  $c_T$ . For motors with neodymium magnets  $c_T$  is approximately equal to  $14,5 \cdot 10^3 [N/m^3]$ . It is consistent with the results estimated in the above considerations – relationship (8).

In paper [4] it has been shown furthermore, that the relationship between the volume  $D^2 L_i$  and the rated torque  $T_N$  of motors using NdFeB magnets can be compared to the same relationship in the case of modern induction motors. Therefore, it is a good basis for the preliminary selection of the main dimensions of the motor made of this type of magnets. When using ferrite magnets (curve 2, Fig.1.) constant  $c_T \approx 4,8 \cdot 10^3 [N/m^3]$ .

Residual magnetic flux density (remanence)  $B_r$  of modern anisotropic ferrite materials is approximately 0,4 T and average remanence of neodymium magnets  $B_r \approx 1,2$  T. If it is assumed that the length of the magnets is chosen according to their coercive force  $H_c$  in such a way, that the demagnetizing effect is the same regardless of the type of material, it can be assumed that the constant  $c_T$  is proportional to the material remanence and approximately is equal:  $c_T \cong 12 \cdot 10^3 \cdot B_r [N/m^3]$ .

Second parameter determining main stator dimension is slenderness ratio  $\lambda_L = L_i / D$ . Slenderness ratio of the designed machines increases with the increase of torque. This means that more torque is achieved by increasing the length  $L_i$  of the machine, not its diameter  $D$ . This is due to mechanical constraints, but also due to the tendency to reduce the moment of inertia. Furthermore, for the machines with larger slenderness ratio, winding ends are shorter and their share in the total winding mass, resistance and power losses is significantly lower. Relationship  $\lambda_L = f(T_N)$  is shown in Fig.2.

Another important stator dimension is the external diameter  $D_z$ . The ratio  $D_z / D = k_D$  of outer and inner diameters of the AC machines stator depends on the rated voltage  $U_N$  and on the number  $p$  of pole pairs [1]. In case of low voltage machines with number of pole pairs  $p = 1, 2, 3, 4$ , the ratio  $k_D = 1,4 \div 1,7$ . In case of high voltage motors the ratio  $k_D = 1,5 \div 1,75$  (the greater values refers to the machines with smaller number of poles) [1].



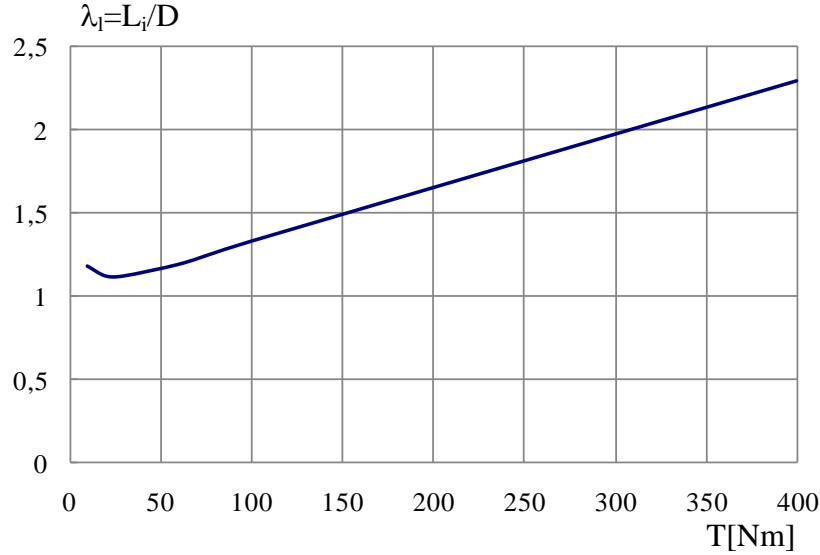


Fig. 8. Dependence of slenderness ratio on required rated torque

Based on the data presented in Fig. 7 and Fig. 8 the following main dimension can be pre-estimated for required rated torque  $T_N$  :

- internal diameter of the stator: 
$$D = \sqrt[3]{\frac{V_w}{\lambda_L}} = \sqrt[3]{\frac{T_N}{c_T \lambda_L}} \cong 0,044 \cdot \sqrt[3]{\frac{T_N}{B_r \lambda_L}}$$
- stator core length: 
$$L_i = \lambda_L D$$
- external diameter of the stator: 
$$D_z = k_D D$$
- external diameter of the rotor: 
$$D_w = D + 2\delta$$

Above dimensions, as well as the air gap width  $\delta$ , can be corrected during recursive design process. Moreover, parameters:  $D$ ,  $L_i$ ,  $\delta$ ,  $\lambda_L$  and  $k_D$  are usually the most important elements of the set of design variables in motor optimizing process.

## 6. The initial selection of the magnet dimensions

Various designs of the rotor are used in permanent magnet electrical machines [2, 3, 8]. Their classification results from the direction of magnetization of the magnets and the method of the magnet mounting. There are two major groups of the motors: (a) with radial magnetization, (b) with circumferential magnetization. An algorithm for the dimension selection of the magnet in the shape of a ring segment is presented. Such shape can be taken as an initial estimate in the finding process of the optimal shape and dimensions of the magnets.

Magnet arc width  $b_m$  derives from the diameter  $D$  and the number of the pole pairs. Equivalent, resultant length  $l_m$  of the magnets (i.e. length in the direction of magnetization) forming pair of poles results from an external circuit reluctance and the maximum demagnetizing magneto-motive force (ampere-turns). Due to the very high coercive forces of the modern ferrite magnets and rare-earth magnets, the demagnetization curve is essentially a straight line. Their relative permeability:  $\mu_w \approx 1,01 \div 1,1$ . In order to determine the working point of the magnet, an algorithm and computer software were developed.

In the analysis, it is convenient to describe the states of the system magnet-external circuit coordinates:  $V_\mu = H \cdot l_m$  and  $\Phi = B \cdot S_m = B \cdot b_m L_i$ . In the absence of the external demagnetizing ampere-turns the working point is the point of intersection of the magnet demagnetizing curve and mirror of the external circuit magnetizing characteristic  $\Phi = f(V_\mu)$ . However, in the case of the existence of the external demagnetizing force  $\Theta_z$ , shifted characteristic  $\Phi = f(V_\mu - \Theta_z)$  must be taken into account – Fig. 9.

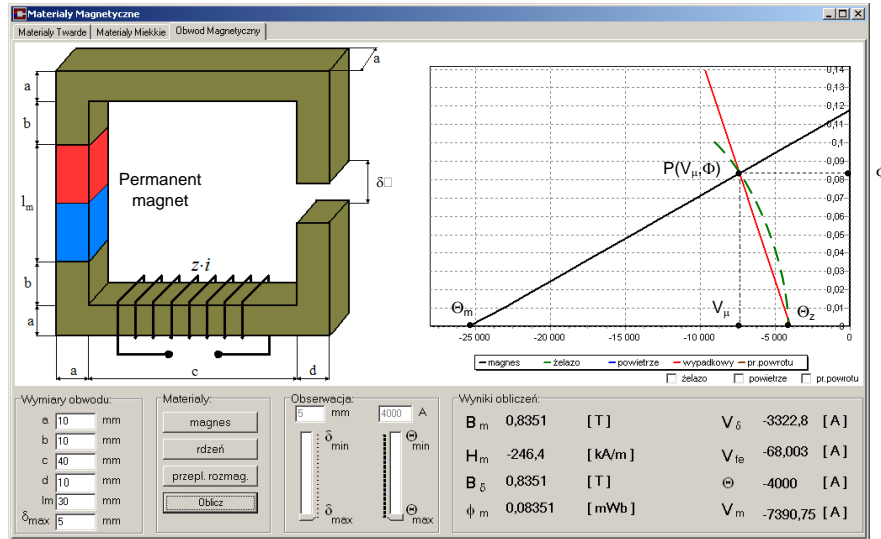


Fig. 9. Determination of the working point of the permanent magnet with demagnetizing magneto-motive force

The main part of the overall reluctance of the machine magnetic circuit is reluctance  $R_{\mu\delta}$  of the air gap. In the preliminary calculations, the ampere-turns drop in the ferromagnetic parts of stator core can be calculated by using so-called saturation factor  $k_{ns} = 1 + V_{\mu Fe} / V_{\mu\delta}$  where  $V_{\mu Fe}$  is a sum of ampere-turn drops in the core. This approach comes down to replacement of magnetic circuit of the stator with equivalent (resultant) air gap width  $\delta' = 2k_c k_{ns} \delta$ , where  $k_c$  is so called Carter's coefficient [1, 4].

Assuming therefore, an alternative, simplified structure of the magnetic circuit in the form presented in Fig. 9, the coordinates  $V_\mu, \Phi$  of the intersection of both characteristics can be easily determined, i.e. the coordinates of the magnet working point. After being divided by  $l_m$  and  $S_m$  respectively, the coordinates  $H, B$  of the magnet working point can be calculated:

$$H = - \frac{\Phi_r + \frac{\mu_0 S_m}{\delta'} \Theta_z}{\mu_0 \mu_w S_m \left( 1 + \frac{l_m}{\delta'} \frac{1}{\mu_w} \right)} \quad (9)$$

$$B = \left( 1 - \frac{1}{1 + \frac{l_m}{\delta'} \frac{1}{\mu_w}} \right) \cdot B_r - \frac{\frac{\mu_0}{\delta'} \Theta_z}{1 + \frac{l_m}{\delta'} \frac{1}{\mu_w}} \quad (10)$$

The magneto-motive force of the stator pole pair depends on the dimensions of the machine and the number of poles:  $\Theta_z = a_z \tau = a_z \pi D / 2p$ , where  $a_z$  is the average specific electric loading in A/m [1, 3],  $\tau$  is the pole pitch. On this basis, the length of the magnet which ensures the postulated magnetic flux density of value  $B$  can be estimated as follows:

$$l_m = \frac{\delta'}{\mu_w} \left( \frac{B_r}{B_r - B} - 1 \right) + \frac{\mu_0 \pi D a_z}{\mu_w p (B_r - B)} \quad (5)$$

At no load operation, the average magnetic flux density in the air gap is of order of 90 % of remanence  $B_r$ . It means that if the reaction of the stator is omitted the length of the magnets should be taken as follows  $l_m \approx (8 \div 9) \delta'$ .

In order to estimate the influence of the stator field,  $\mu_w \cong 1$  and  $l_m / \delta' = 8$  have been assumed. With the omission of demagnetizing ampere-turns the flux density  $B_0 = 0,89B_r$ . However, taking into account the demagnetizing stator reaction, based on assumption:  $B_r = 1,2 \text{ T A/m}$ ;  $a_z = 20 \text{ kA/m}$ ,  $D = 10 \text{ cm}$  and  $p = 4$  the following result is obtained:  $B = 0,85B_r$ . In the case of large machines with a small number of pole pairs, the stator field impact on the magnets working point is significantly larger. For example, if  $p = 2$  the magnetic flux density decreases to the value  $B = 0,82B_r$ , and if  $p = 1$  – to the value  $B = 0,74B_r$ . Specific electric loading in high power machines can exceed 50 kA/m. If  $a_z = 40 \text{ kA/m}$ , for  $p = 1$  magnetic flux density in loaded motor decreases to  $B = 0,6B_r$ . Omission of the influence of the stator field reaction on the magnet working point, where magnet length was selected according to no load state, might result in considerable errors.

If the reaction of the stator field is neglected, the magnet length should be selected in proportion to the length of the equivalent air gap:  $l_m = k_m \delta'$ . In the case of machines with larger power output, especially the machines with two poles, taking stator reaction into account, the coefficient  $k_m$  should be selected from the range  $10 \div 20$ .

## 7. Selection of the motor parameters in terms of cogging torque minimization

The initial design of the stator requires: selection of slots number, selection of shape and slots dimensions, determination of the yoke dimension and selection of the type and basic parameters of winding.

Due to the expected motor electromagnetic parameters and the possibility of using more types of windings, the stator slots number  $N_s$  should be as great as possible. Increase in number of slots is of course associated with an increase in manufacturing cost. However, the more important restrictions arise from the need to limit the slot leakage magnetic flux and the cost of slot insulation. For example, the width of the slot  $b_s$  in the machines with voltages 500 and 1000 V shall not be less than approx.  $8 \div 14 \text{ mm}$ , in the machines with voltage 6000 V –  $10,5 \div 16 \text{ mm}$  (larger values are related to machines with a higher pole pitch) [1]. In order to estimate the number of the slots in these two cases, the average values  $b_s \approx 10$  and  $b_s \approx 13 \text{ mm}$  have been assumed.

Assuming an optimum ratio  $k_s$  of slot ending width  $b_s$  to the slot pitch  $t$  in the range  $0,4 \leq k_s \leq 0,5$  (lower value applies to high power machines [1]) the following stator parameters can be pre-determined:

- number of stator slots:  $N_s = k_s \frac{\pi D}{b_s}$
- slot pole pitch:  $t = \pi D / N_s$
- number of slots per pole and phase:  $q = \frac{N_s}{2mp}$

Fractional number of slots per pole and phase can be obtained as a result of use of winding consisting of at least two different groups of coils.

In the case of permanent magnet motors, generation of an additional reluctance torque (cogging torque) is one of the most important problems. Reluctance torque is a result of change of the number of teeth within one pole pitch during rotation, in other words, due to the change of equivalent air-gap reluctance within one magnet pole. The cogging torque causes the electromagnetic torque pulsation and hinders the motor start-up.

The cogging torque can be greatly reduced by the use of skewed stator slots or slanted rotor magnets, but this obviously will increase the cost of motor manufacturing. Significant reduction or even elimination of the cogging torque can be achieved by proper selection of the number of slots in the stator and the magnet pole span in the rotor. The optimal relations between numbers of pole pairs and the number of stator slots, taking the minimum cogging torque into account, are summarized in Table 1 [6].

Table 1. The optimal relations between number of pole pairs and the number of slots in permanent magnet synchronous machines

Number of pole pairs $p$	Number of slots								
	$q = 1$	$q = 1\frac{1}{4}$	$q = 1\frac{1}{2}$	$q = 1\frac{3}{4}$	$q = 2$	$q = 2\frac{1}{2}$	$q = 3$	$q = 3\frac{1}{2}$	$q = 4$
<b>1</b>	6	-	9	-	12	-	18	-	24
<b>2</b>	12	15	18	21	24	24	36	42	48
<b>3</b>	18	-	27	-	36	-	54	-	72
<b>4</b>	24	30	36	42	48	60	60	84	96

In order to quantify above relations, the software supporting optimal selection of the number of slots in relation to the number of pole pairs was developed. The minimum cogging torque has been taken as criterion.

Two-dimensional (2D) field model of the electromagnetic phenomena has been applied. The structures of the selected permanent magnet synchronous machines were examined [3, 6]. A number of calculations have been made for the number of pole pairs  $p = 1, 2, 3$ , and the number  $q$  of slots per pole and phase in range  $1 \div 3$ , including fractional  $q$ .

In the calculation two design variables has been assumed:

- pole pitch cover coefficient  $k_\tau = b_m / \tau$ ,
- relative slot opening width  $k_t = b_s / t$ .

Maximum absolute value of cogging torque  $T_{z\max} = \max_\alpha |T_z(\alpha)|$ , were the rotor turning angle  $\alpha$  interval corresponds to one slot pitch, has been assumed as a comparative criterion.

Below are presented sample results of calculations for the classic salient pole-shoe permanent magnet synchronous motor (Fig. 4) with the following parameters: diameter  $D = 94$  mm, length  $L_i = 125$  mm, number of pole pairs  $p = 2$  ( $\tau = 73,83$  mm), number of stator slots  $N_s = 36$  ( $q = 3, t = 8,2$  mm), the pole pitch cover coefficient  $k_\tau = b_m / \tau = 0,56$  and relative slot opening width  $k_t = b_s / t = 0,4$ .

Figure 10 illustrates the dependence of the cogging torque on the rotor angle  $\alpha$  (green axis) and on the pole pitch cover ratio  $k_\tau$  (blue axis) for two values of the relative slot opening width (a)  $k_t = 0,4$  i (b)  $k_t = 0,5$ . Graphs has been drawn for the range of angle changes  $\alpha \in (0, 10^\circ)$  and for  $k_\tau \in (0,2 \div 0,86)$ .

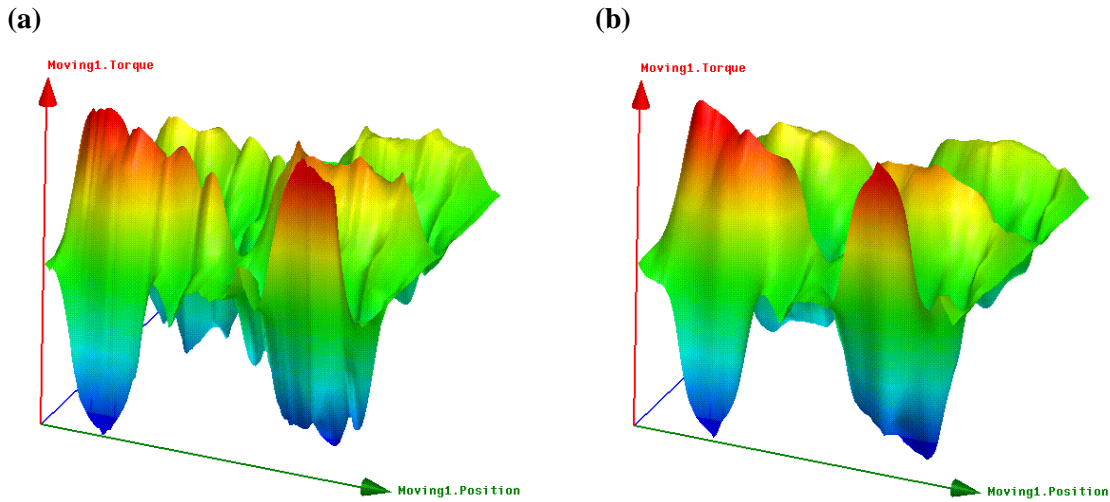


Fig. 10. Dependence of cogging torque on rotor angle  $\alpha$  and on pole pitch cover factor  $k_\tau$  for: (a)  $k_t = 0,4$  and (b)  $k_t = 0,5$

Figure 11 shows the relations between the maximum absolute value of cogging torque  $T_{c\text{omax}}$  (assumed as a comparative criterion) and relative width of the pole  $k_\tau = b_m/\tau$  for five values of relative slot opening width  $k_t = b_s/t$ . This Figure shows that the cogging torque strongly depends on the relation between dimensions of the rotor pole and number and dimension of the stator slots and teeth. In the considered case, the cogging torque minimum corresponds to pole pitch cover  $k_\tau = 0.66$ ; the cogging torque is almost four times smaller than for motor with relative pole width  $k_\tau = 0.70$  and up to six times smaller than for  $k_\tau = 0.58$ .

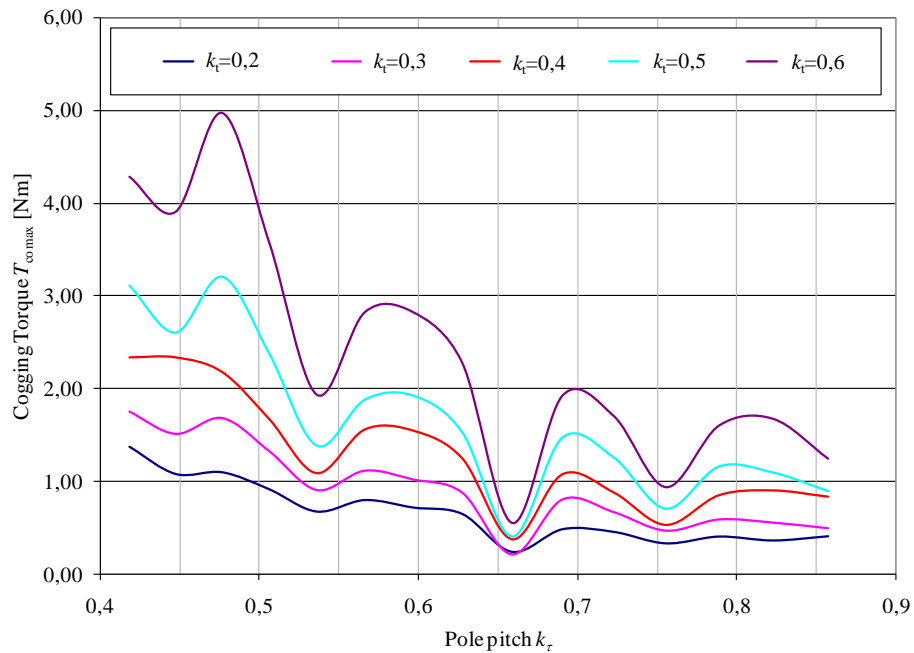


Fig. 11. Dependence of cogging torque on the pole pitch covering  $k_\tau$  and relative slot ending width  $k_t$

In the optimal design process the genetic algorithm can be used. The number of slots will be the coordinating variable in this process, while the relative sizes:  $k_\tau = b_m/\tau$ ,  $k_{t1} = b_{s1}/t$  and  $k_{t2} = b_{s2}/t$  will be the continuous design variables.

## 5. Conclusions

The developed software allowing to determine the optimal working point of fan or pump system can be used in the design of efficient driving motors. It also allows to determine the load characteristics, which can be used in the design of the engine control system.

The convergence of the optimization procedure strongly depends on the selection of the proper dimensions of the device initial variants. Presented algorithm for selection of the permanent magnet synchronous motors main dimensions can be used for defining the set of initial points in the optimization processes. Elaborated software for the determination of the permanent magnet working point can be helpful in the synchronous and brushless direct current motors design. The another computer software can be used to support the design process of the magnetic circuit, taking the minimization of the cogging torque into considerations. It allows to determine the optimal rotor pole and stator slots dimensions.

## References

### Art 1 (Proszę przetłumaczyć tytuły na angielski dodając w nawiasie (in Polish))

- [1] Gundlach W. R., Podstawy maszyn przepływowych i ich systemów energetycznych, WNT, Warszawa, 2008.
- [2] Jędrał W., Pompy wirowe, Warszawa, Wydawnictwo Naukowe PWN, 2001.
- [3] Katalog firmy Flygt: Pompy odwadniające. Pompy dla przemysłu górniczego. <http://www.ittwww.pl/>, 06.05.2010.
- [4] Stępniewski M, Pompy, WNT, Warszawa, 1985.
- [5] Szklarski L., Skalny A., Strycharz J., Dynamika i sterowanie stacjonarnych napędów elektrycznych w górnictwie, PWN, Warszawa, 1984.

### Art 2

- [6] Dąbrowski M., Design of alternating current electrical machines (in Polish), WNT, Warszawa 1994.
- [7] Ferreti G. Magnani C., Rocco P., Modelling, identification and compensation of pulsating torque in permanent magnet AC motors, IEEE Trans. on Industrial Electronics, Vol. 45 No. 6, 1998, s. 912-920.
- [8] Gieras J.F., Wing M., Permanent magnet motor technology - design and application, Marcel Dekker, 2002.
- [9] Glinka T., Permanent magnet electrical machines (in Polish), Wyd. Politechniki Śląskiej, Gliwice, 2002.
- [10] Hafner M., Schoning M., Hameyer K., Automated sizing of permanent magnet synchronous machines with respect to electromagnetic and thermal aspects, COMPEL-The international journal for computation and mathematics in electrical and electronic engineering, Vol29, No 5, 2010.
- [11] Hendershot J.R., Miller T.J.E., Design of Brushless Permanent-Magnet Motors, Magna Physics Publishing and Clarendon Press, Oxford, 1994.
- [12] Wing M., Analysis of an energy efficient permanent magnet brushless universal motor, D. Ph. Thesis, Department of Electrical Engineering, University of Cape Town (RSA), February 1996.